

Green's Function and Receptance for Structures Consisting of Beams and Plates

K. Kelkel*

University of Darmstadt, Darmstadt, Federal Republic of Germany

Expressions for Green's function of the free rectangular plate and structures consisting of beams and plates are derived by analytical and semianalytical methods to be used in a distributed element program. Thereby, the boundary-value problem for the forced vibrations of the free plate excited harmonically by a concentrated load at an arbitrary point is divided into three appropriate plate problems, with solutions of the Levy-type. Then, Green's functions for structures being more complex are gained using the substructure technique, whereby Green's functions of the free substructures are taken as basis. Using the superposition principle, they can be reduced to Green's functions for simpler boundary conditions. Green's function for the whole structure then yields the receptance matrices for arbitrary connecting points.

I. Introduction

ONE method of deriving a linear dynamical model for a complex system is to describe the dynamics of its subsystems by means of certain input-output relations, which can, for example, be dynamic stiffness or dynamic compliance (receptance) matrices.¹ The elements of the latter matrices correspond to special values of Green's function, i.e., Green's function yields the receptance matrices for arbitrary connecting points. Subsequently, these compliances will be related to each other in order to model the full structure.

This procedure is called the exact displacement method, and was developed for frames in the early 1940's by Koulousek.² Important progress enhancing the applicability of the exact displacement method was made in 1970 through the algorithm of Wittrick and Williams³ for the automatic calculation of natural frequencies. In 1976, Åkesson⁴ developed a distributed element computer program dedicated to frame structures. Seven years later, Poelaert⁵ presented ESTEC's distributed element package DISTEL, which allows for dynamic and response analysis of three-dimensional arbitrary configurations composed of beams, rectangular membranes, extensive strings, and rigid bodies with an arbitrary number of connection points.

To extend the preceding distributed programs, the rectangular plate is handled in this paper. Let us consider the free-body diagram of the structure shown in Fig. 1, which consists of a free rectangular plate reinforced along one edge by a beam. We have for subsystems: the rectangular plate, the transverse beam, and the torsion bar. Our first task is the calculation of the corresponding Green's functions, which can be found in the literature for the bar and beam. Nevertheless, the calculation for the transverse beam is given here in detail to familiarize the reader with the basic ideas of the recent calculation of Green's function for the free rectangular plate.⁶

II. Green's Function for the Free Transverse Beam

Green's function $G^f(x, \xi, \omega)$ for the free transverse beam represents the vibrational amplitude $W(x)$ of the beam excited by a unit force at $x = \xi$ oscillating harmonically with frequency ω . The calculation can be simplified if we divide the load into one symmetric and one antisymmetric part, as shown in Fig. 2.

A. Antisymmetric Part

For the beam loaded antisymmetrically, the deflection and the bending moment must vanish at $x = 0$, i.e., it is sufficient to consider the half-beam with a hinged end at $x = 0$. Second, we divide the problem into two "building blocks" to simplify the boundary conditions by exchanging dynamical boundary conditions for geometrical ones. We can proceed in two different ways: Either we choose the vanishing slope or we choose vanishing deflection at $x = a$. Corresponding to our choice, we must then add a second building block, a bending moment at $x = a$, as done in Sec. II. B for the symmetric part of the load, following the middle column of Fig. 2, or a vanishing transverse force, as done in this section, following the right column of Fig. 2. That is, the calculation of Green's function G^f for the free substructure is reduced to the simpler calculation of Green's function G^h for the

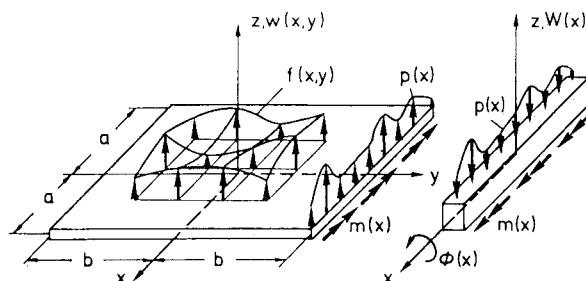


Fig. 1 Free rectangular plate reinforced by a beam.

Received April 1, 1986; presented as Paper 86-0927 at the AIAA/ASME/ASCE/AHS 27th Structures, Structural Dynamics and Materials Conference, San Antonio, TX, May 19-21, 1986; revision received Feb. 2, 1987. Copyright © American Institute of Aeronautics and Astronautics, Inc., 1987. All rights reserved.

*Privatdozent, Institut für Mechanik, Department of Mechanics.

substructure with hinged supports

$$G^h(x, \xi) = \frac{a^3}{2EI\eta^3} \left[-\frac{\sinh\eta [1 - (\xi/a)]}{\sinh\eta} \sinh\eta \frac{x}{a} + \frac{\sinh\eta [1 - (\xi/a)]}{\sinh\eta} \sinh\eta \frac{x}{a} + \left(\sinh\eta \frac{x-\xi}{a} - \sinh\eta \frac{x-\xi}{a} \right) u(x-\xi) \right]; \quad \eta = a\sqrt{\frac{\mu\omega^2}{EI}} \quad (1)$$

where EI denotes the flexural stiffness, μ the mass per unit length of the beam, and $u(*)$ the unit step function. For $(\xi/a) = 1/2$, the absolute value of $G^h(x, \xi, \eta)$ is shown in Fig. 3.

For the second building block, we have to solve the boundary value problem

$$W_a^{F''''}(x) - \left(\frac{\eta}{a}\right)^4 W_a^F(x) = 0$$

$$W_a^F(0) = W_a^{F''}(0) = 0, \quad W_a^F(a) = 0$$

$$W_a^{F'''}(a) = -\frac{F}{EI} = -\frac{1}{2} \frac{\partial^3}{\partial x^3} G^h(a, \xi) \quad (2)$$

Therein, the last condition guarantees the disappearance of the transverse force at the ends of the beam. Using Eq. (1), for the antisymmetric part of Green's function for the free transverse beam we finally get

$$G_a^f(x, \xi) = \frac{a^3}{4EI\eta^3} \left[\left(\frac{\sinh\eta(\xi/a) + (\text{chc} - \text{shs})\sinh\eta(\xi/a)}{\text{shc} - \text{chs}} - \cosh\eta \frac{\xi}{a} \right) \sinh\eta \frac{x}{a} + \left(\frac{\sinh\eta(\xi/a) + (\text{chc} + \text{shs})\sinh\eta(\xi/a)}{\text{shc} - \text{chs}} + \cos\eta \frac{\xi}{a} \right) \times \sinh\eta \frac{x}{a} + \left(\sinh\eta \frac{x-\xi}{a} - \sinh\eta \frac{x-\xi}{a} \right) u(x-\xi) \right] \quad (3)$$

where

$$\text{ch} = \cosh\eta, \quad \text{sh} = \sinh\eta, \quad \text{c} = \cos\eta, \quad \text{s} = \sin\eta \quad (4)$$

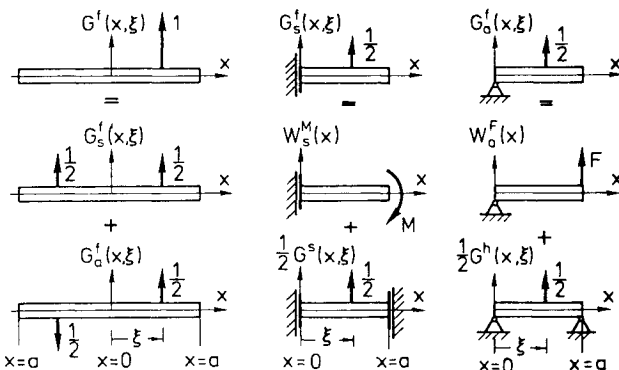


Fig. 2 Separation of the Green's function for the transverse beam in one symmetric and one antisymmetric part; building blocks for analyzing both parts.

B. Symmetric Part

For the beam loaded symmetrically, the slope and the transverse force must vanish at $x=0$, i.e., it is sufficient to consider the half-beam with so-called "slip shear" conditions at $x=0$. For building blocks, we can now choose Green's function G^s for the substructure with slip shear conditions at the ends

$$G^s(x, \xi) = \frac{a^3}{2EI\eta^3} \left[-\frac{\cosh\eta [1 - (\xi/a)]}{\sinh\eta} \cosh\eta \frac{x}{a} - \frac{\cos\eta [1 - (\xi/a)]}{\sinh\eta} \cos\eta \frac{x}{a} + \left(\sinh\eta \frac{x-\xi}{a} - \sinh\eta \frac{x-\xi}{a} \right) u(x-\xi) \right] \quad (5)$$

and the solution of the boundary-value problem

$$W_s^{M''''}(x) - \left(\frac{\eta}{a}\right)^4 W_s^M(x) = 0$$

$$W_s^{M'}(0) = 0, \quad W_s^{M'''}(0) = W_s^{M'''}(a) = 0$$

$$W_s^{M''}(a) = -\frac{M}{EI} = -\frac{1}{2} \frac{\partial^2}{\partial x^2} G^s(a, \xi) \quad (6)$$

Here, the last condition guarantees the disappearance of the bending moment at the ends of the beam. For the symmetric part of Green's function of the free transverse beam, we then have with Eq. (5)

$$G_a^f(x, \xi) = \frac{a^3}{4EI\eta^3} \left[\left(\frac{\sinh\eta(\xi/a) + (\text{chc} - \text{shs})\sinh\eta(\xi/a)}{\text{shc} - \text{chs}} - \sinh\eta \frac{\xi}{a} \right) \cosh\eta \frac{x}{a} - \left(\frac{\cosh\eta(\xi/a) + (\text{chc} - \text{shs})\cosh\eta(\xi/a)}{\text{chs} + \text{shc}} + \sinh\eta \frac{\xi}{a} \right) \times \cos\eta \frac{x}{a} + \left(\sinh\eta \frac{x-\xi}{a} - \sinh\eta \frac{x-\xi}{a} \right) u(x-\xi) \right] \quad (7)$$

and for the whole Green's function

$$G^f(x, \xi) = G_s^f(x, \xi) + G_a^f(x, \xi) \quad (8)$$

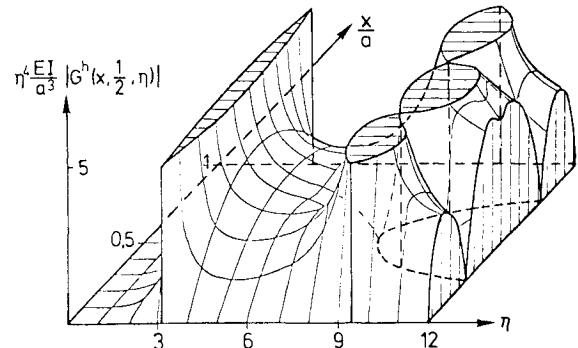


Fig. 3 Absolute value of the Green's function of a beam with hinged supports.

III. Green's Function for the Free Rectangular Plate

A rectangular plate with free boundaries has two lines of symmetry, which correspond to the x and y axes, respectively. Now, if we split up the amplitude $f(x,y)$ of the exciting force per unit area (see Fig. 1) in one double symmetric, two symmetric-antisymmetric, and one double antisymmetric, which is possible for every function $f(x,y)$, the corresponding vibrations will have the same properties of symmetry:

$$\Delta^2 w_{ij}(x,y) - \left(\frac{\bar{\eta}}{a}\right)^4 w_{ij}(x,y) = \frac{1}{D} f_{ij}(x,y) \quad (9)$$

$$i,j \in (s,a), \quad \Delta = \frac{\partial^2}{\partial x^2} + \frac{\partial^2}{\partial y^2}, \quad \bar{\eta} = a\sqrt{\frac{\bar{\mu}\omega^2}{D}}$$

$$\begin{aligned} w_{ss}(x,y) &= w_{ss}(x,-y) = w_{ss}(-x,y) \\ w_{sa}(x,y) &= -w_{sa}(x,-y) = w_{sa}(-x,y) \\ w_{as}(x,y) &= w_{as}(x,-y) = -w_{as}(-x,y) \\ w_{aa}(x,y) &= -w_{aa}(x,-y) = -w_{aa}(-x,y) \end{aligned} \quad (10)$$

the whole deflection of the plate being

$$w(x,y) = w_{ss}(x,y) + w_{sa}(x,y) + w_{as}(x,y) + w_{aa}(x,y) \quad (11)$$

Thereby D denotes the flexural stiffness and $\bar{\mu}$ the mass per unit area of the plate. Due to symmetry, for each one of the preceding four parts of the load, only a quarter segment of the fully free plate need be analyzed. If we choose for $f(x,y)$ a concentrated load at an arbitrary point (ξ,ρ)

$$f(x,y) = \delta(x-\xi, y-\rho) \quad (12)$$

wherein, $\delta(*,*)$ denotes the "two-dimensional" delta distribution, the corresponding $w(x,y)$ marks Green's function $g^f(x,y,\xi,\rho)$, as shown in Fig. 4.

A. Antisymmetric-Symmetric Part

In this case, Eq. (10) gives

$$w(x,y) = -w(-x,y), \quad \frac{\partial}{\partial y} w(x,y) = -\frac{\partial}{\partial y} w(x,-y) \quad (13)$$

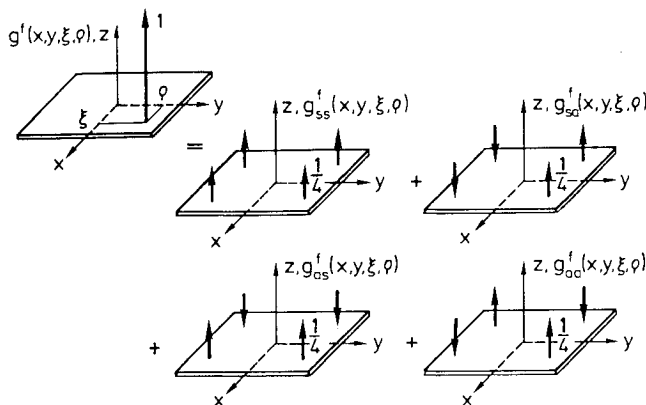


Fig. 4 Separation of the Green's function in symmetric and antisymmetric parts.

$$\mathfrak{M}_x w(x,y) = -\mathfrak{M}_x w(-x,y), \quad \nabla_y w(x,y) = -\nabla_y w(x,-y) \quad (14)$$

$$\begin{aligned} \mathfrak{M}_n &= -D \left(\frac{\partial^2}{\partial n^2} + \nu \frac{\partial^2}{\partial s^2} \right) \\ \nabla_n &= -D \frac{\partial}{\partial n} \left(\frac{\partial^2}{\partial n^2} + (2-\nu) \frac{\partial^2}{\partial s^2} \right) \quad n,s \in (x,y), \quad n \neq s \end{aligned} \quad (15)$$

and, therefore, also

$$w_{as}(0,y) = 0, \quad M_x(0,y) = \mathfrak{M}_x w_{as}(0,y) = 0 \quad (16)$$

we have no deflection and external bending moment M_x at $x=0$, i.e., hinged support, and

$$\frac{\partial}{\partial y} w_{as}(x,0) = 0, \quad V_y(x,0) = \nabla_y w_{as}(x,0) = 0 \quad (17)$$

we have no slope and "effective transverse force" V_y at $y=0$, i.e., slip shear conditions (see Fig. 5).

Now, we have to separate the problem into three building blocks, following Fig. 5, to reduce it to the simpler problem of the calculation of Green's function g^s for the structure with slip shear conditions

$$g^s(x,y,\xi,\rho) = \sum_{m=0}^{\infty} \sum_{n=0}^{\infty} 4F_{mn} W_m^s(x) W_m^s(\xi) U_n^s(y) U_n^s(\rho) \quad (18)$$

$$F_{mn} = \frac{a^3}{4Db} \frac{1}{(m^2 + \phi^2 n^2)^2 (\pi/2)^4 - \bar{\eta}^4}, \quad \phi = \frac{a}{b}$$

$$W_m^s(x) = 1, \quad m=0$$

$$= \sqrt{2} \cos \frac{m}{2} \pi \frac{x}{a}, \quad m \in N_s \setminus \{0\} = \{2,4,\dots,\infty\}$$

$$= \sqrt{2} \sin \frac{m}{2} \pi \frac{x}{a}, \quad m \in N_a = \{1,3,5,\dots,\infty\}$$

$$U_n^s(y) = W_n^s\left(\frac{a}{b} y\right) \quad (19)$$

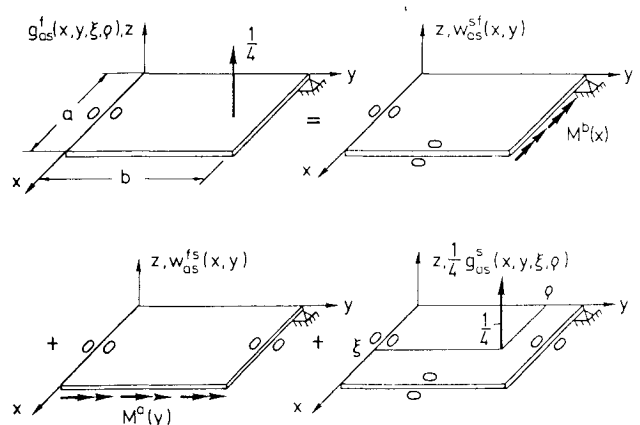


Fig. 5 Building blocks for analyzing the antisymmetric-symmetric part of the Green's function for the free rectangular plate.

For the four classes of symmetry, we then have

$$g_{ij}^s(x, \xi, y, \rho) = \sum_{n \in N_i} \sum_{n \in N_j} 4F_{mn} W_m^s(x) W_m^s(\xi) U_n^s(y) U_n^s(\rho) \quad i, j \in \langle s, a \rangle \quad (20)$$

For the second building block in Fig. 5, we have to solve the boundary-value problem

$$\begin{aligned} \Delta^2 w_{as}^{sf}(x, y) - \left(\frac{\bar{\eta}}{a}\right)^4 w_{as}^{sf}(x, y) &= 0 \\ \frac{\partial}{\partial x} w_{as}^{sf}(a, y) &\equiv 0, \quad \nabla_x w_{as}^{sf}(a, y) \equiv 0 \\ \nabla_y w_{as}^{sf}(x, b) &\equiv 0, \quad \mathfrak{M}_y w_{as}^{sf}(x, b) = M^b(x) \end{aligned} \quad (21)$$

and, in addition, Eqs. (16) and (17) with w_{as}^{sf} for w_{as} . The solution can be expressed in the form proposed by Levy as

$$w_{as}^{sf}(x, y) = \sum_{m \in N_a} W_m^s(x) U_{sm}^f(y) \quad (22)$$

when the external moment M_b is developed in Fourier series as

$$M^b(x) = \sum M_m^b W_m^s(x) \quad (23)$$

For the "beam function" $U_{sm}^f(y)$, then we get an ordinary boundary-value problem of fourth order. Its solution has the form⁶

$$U_{sm}^f(y) = M_m^b Y_{sm}(y) \quad (24)$$

$$\begin{aligned} Y_{sm}(y) &= -\frac{a^2}{D} \frac{1}{N_{sm}^b} \left(\frac{u_m^+ \cosh s_m^+(y/b)}{s_m^+ \sinh s_m^+} + \frac{u_m^-}{s_m^-} \operatorname{ctgh} s_m^- \frac{y}{b} \right) \\ N_{sm}^b &= \frac{1}{s_m^+} u_m^{+2} \operatorname{cths} s_m^+ - \frac{1}{s_m^-} u_m^{-2} \operatorname{ctgh} s_m^- \end{aligned} \quad (25)$$

$$s_m^+ = \frac{b}{a} \sqrt{\left| \bar{\eta}^2 \pm \left(m \frac{\pi}{2} \right)^2 \right|}, \quad u_m^+ = \bar{\eta}^2 \pm (1 - \nu) \left(m \frac{\pi}{2} \right)^2 \quad (26)$$

$$\begin{aligned} \operatorname{ctgh} s_m^- \frac{y}{b} &= \frac{\cosh s_m^-(y/b)}{-\sinh s_m^-}, \quad m \in N^{a-} = \langle 0, 1, \dots, \bar{m} \leq \frac{2\bar{\eta}}{\pi} < \bar{m} + 1 \rangle \\ &= \frac{\cosh s_m^-(y/b)}{\sinh s_m^-}, \quad m \in N^{a+} = \langle \bar{m} + 1, \bar{m} + 2, \dots, \infty \rangle \end{aligned}$$

$$\operatorname{ctgh} s_m^- = \operatorname{ctgh} s_m^- \frac{y}{b} \Big|_{y=b} \quad (27)$$

For the third building block, we have

$$\begin{aligned} \Delta^2 w_{as}^{fs}(x, y) - \left(\frac{\bar{\eta}}{a}\right)^4 w_{as}^{fs}(x, y) &= 0 \\ \frac{\partial}{\partial y} w_{as}^{fs}(x, b) &\equiv 0, \quad \nabla_y w_{as}^{fs}(x, b) \equiv 0 \\ \nabla_x w_{as}^{fs}(a, y) &\equiv 0, \quad \mathfrak{M}_x w_{as}^{fs}(a, y) = M^a(y) \end{aligned} \quad (28)$$

and, in addition, Eqs. (16) and (17) with w_{as}^{fs} for w_{as} , with the solution⁶

$$w_{as}^{fs}(x, y) = \sum_{n \in N_s} W_{an}^f(x) U_n^s(y) \quad (29)$$

$$M^a(y) = \sum_{n \in N_s} M_n^a U_n^s(y) \quad (30)$$

$$W_{an}^f(x) = M_n^a X_{an}(x) \quad (31)$$

$$\begin{aligned} X_{an}(x) &= \frac{b^2}{D} \frac{1}{N_{an}^a} \left(\frac{v_n^+ \sinh t_n^+(x/a)}{t_n^+ \cosh t_n^+} + \frac{v_n^-}{t_n^-} \operatorname{tgh} t_n^- \frac{x}{a} \right) \\ N_{an}^a &= \frac{1}{t_n^-} v_n^{+2} \operatorname{tgh} t_n^- - \frac{1}{t_n^+} v_n^{-2} \operatorname{th} t_n^+ \end{aligned} \quad (32)$$

$$t_n^+ = \sqrt{\left| \bar{\eta}^2 \pm \left(\phi n \frac{\pi}{2} \right)^2 \right|}, \quad v_n^+ = \bar{\eta}^2 \pm (1 - \nu) \left(\phi n \frac{\pi}{2} \right)^2 \quad (33)$$

$$\begin{aligned} \operatorname{tgh} t_n^- \frac{x}{a} &= \frac{\sinh t_n^-(x/a)}{\cosh t_n^-}, \quad n \in N^{b-} = \langle 0, 1, \dots, \bar{n} \leq \frac{2\bar{\eta}}{\phi\pi} < \bar{n} + 1 \rangle \\ &= \frac{\sinh t_n^-(x/a)}{\cosh t_n^-}, \quad n \in N^{b+} = \langle \bar{n} + 1, \bar{n} + 2, \dots, \infty \rangle \\ \operatorname{tgh} t_n^- &= \operatorname{tgh} t_n^- \frac{x}{a} \Big|_{x=a} \end{aligned} \quad (34)$$

Since the solutions of Eqs. (22) and (29) satisfy the homogeneous part of the differential equation (9), and Eq. (20) satisfies the inhomogeneous equation (9) with Eq. (12), the sum

$$g_{as}^f(x, y, \xi, \rho) = w_{as}^{sf}(x, y) + w_{as}^{fs}(x, y) + \frac{1}{4} g_{as}^s(x, y, \xi, \rho) \quad (35)$$

will satisfy the inhomogeneous equation (9). We must, however, constrain the Fourier coefficients in the moment expressions (23) and (30) so that the net effect gives a zero bending moment along the edges $x=a$ and $y=b$. It is easily seen that all other boundary conditions are satisfied.

For the contributions to the bending moment along the edge $x=a$, we have

$$M^a(y) + \mathfrak{M}_x w_{as}^{fs}(a, y) = -\frac{1}{4} \mathfrak{M}_x g_{as}^s(a, y; \xi, \rho) \quad (36)$$

and with Eqs. (19), (20), (22-27), and (30), finally

$$M_n^a + \sum_m A_{nm} M_m^b = f_n^a, \quad f_n^a = \sum_m C_{nm} W_m^s(\xi) U_n^s(\rho) \quad (37)$$

with $m \in N_a$ and $n \in N_s$ for the antisymmetric-symmetric part handled here. With Eqs. (18) and (20), we get for the coefficients C_{nm}

$$\begin{aligned} C_{nm} &= -\sqrt{2}(-1)^{[(m-1)m/2]} \frac{D}{a^2} (m^2 + \nu \phi^2 n^2) \left(\frac{\pi}{2} \right)^2 F_{mn} \quad m \neq 0 \\ C_{n0} &= -\nu \frac{D}{b^2} n^2 \left(\frac{\pi}{2} \right)^2 F_{on} \end{aligned} \quad (38)$$

and with Eqs. (22) and (24),

$$A_{nm} = -(-1)^{[(m-1)m+n]/2} \phi \frac{E_{mn}}{N_{sm}^b}, \quad n \in N_s \quad (39)$$

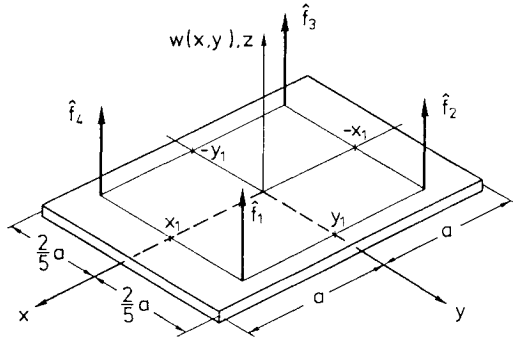


Fig. 6 Free rectangular plate excited by four transverse forces.

$$E_{mn} = 16 \frac{D}{a^2} \bar{\eta}^2 \left[\nu \bar{\eta}^4 + (1 - \nu)^2 m^2 \phi^2 n^2 \left(\frac{\pi}{2} \right)^4 \right] F_{mn} \quad (40)$$

The contributions to the bending moment along the edge $y = b$ are

$$\mathfrak{M}_y w_{as}^{fs}(x, b) + M^b(x) = -\frac{1}{4} \mathfrak{M}_y g_{as}^s(x, b; \xi, \rho) \quad (41)$$

or with Eqs. (19), (20), (23), and (29-34),

$$\sum_n B_{mn} M_n^a + M_m^b = f_m^b, \quad f_m^b = \sum_n D_{mn} W_m^s(\xi) U_n^s(\rho) \quad (42)$$

($m \in N_a$, $n \in N_s$ here). Herein, the coefficients are

$$D_{mn} = -\sqrt{2} (-1)^{[(n-1)n/2]} \frac{D}{a^2} (\nu m^2 + \phi^2 n^2) \left(\frac{\pi}{2} \right)^2 F_{mn}, \quad n \neq 0$$

$$D_{m0} = -\nu \frac{D}{a^2} m^2 \left(\frac{\pi}{2} \right)^2 F_{m0} \quad (43)$$

$$B_{mn} = -(-1)^{[(n-1)n+m+1]/2} \frac{b}{a} \frac{E_{mn}}{N_{sn}^a}, \quad m \in N_a \quad (44)$$

B. Double Symmetric Part

Here we have from Eq. (10) slip shear conditions at $x=0$ and $y=0$, i.e.,

$$\frac{\partial}{\partial x} w_{ss}(0, y) \equiv 0, \quad \nabla_x w_{ss}(0, y) \equiv 0 \quad (45)$$

$$\frac{\partial}{\partial y} w_{ss}(x, 0) \equiv 0, \quad \nabla_y w_{ss}(x, 0) \equiv 0 \quad (46)$$

The further calculation is similar to that in Sec. III A. For results different from the preceding, we have

$$w_{ss}^{fs}(x, y) = \sum_{n \in N_s} W_{sn}^f(x) U_n^s(y) \quad (47)$$

$$W_{sn}^f(x) = M_n^a X_{sn}(x)$$

$$X_{sn}(x) = -\frac{b^2}{D} \frac{1}{N_{sn}^a} \left(\frac{v_n^+ \cosh t_n^+(x/a)}{t_n^+ \sinh t_n^+} + \frac{v_n^-}{t_n^-} \text{ctgh} t_n^- \frac{x}{a} \right) \quad (48)$$

$$N_{sn}^a = \frac{1}{t_n^+} v_n^{+2} \text{cth} t_n^+ - \frac{1}{t_n^-} v_n^{-2} \text{ctgh} t_n^- \quad (49)$$

where $\text{ctgh} t_n^- (x/a)$ is defined as in Eq. (27), s , m , y/b , and a being substituted by t , n , x/a , and b . The final result is

$$M_n^a + \sum_{m \in N_s} A_{nm} M_m^b = U_n^s(\rho) \sum_{m \in N_s} C_{nm} W_m^s(\xi), \quad n \in N_s \quad (50)$$

$$\sum_{n \in N_s} B_{mn} M_n^a + M_m^b = W_m^s(\xi) \sum_{n \in N_s} D_{mn} U_n^s(\rho), \quad m \in N_s \quad (51)$$

with C_{nm} , A_{nm} , and D_{mn} from Eqs. (38), (39), and (43), and with Eqs. (47-49),

$$B_{mn} = -(-1)^{[(n-1)n+m]/2} \frac{b}{a} \frac{E_{mn}}{N_{sn}^a}, \quad m \in N_s \quad (52)$$

C. Double Antisymmetric Part

Therefore, the quarter-plate has hinged support at $x=0$ and $y=0$. For results different from Sec. III A, we now have

$$w_{aa}^{sf}(x, y) = \sum_{m \in N_a} W_m^s(x) U_{am}^f(y) \quad (53)$$

$$U_{am}^f(y) = M_m^b Y_{am}(y)$$

$$Y_{am}(y) = \frac{a^2}{D} \frac{1}{N_{am}^b} \left[\frac{u_m^+ \sinh s_m^+(y/b)}{s_m^+ \cosh s_m^+} + \frac{u_m^-}{s_m^-} \text{tgh} s_m^- \frac{y}{b} \right] \quad (54)$$

$$N_{am}^b = \frac{1}{s_m^-} u_m^{-2} \text{tgh} s_m^- - \frac{1}{s_m^+} u_m^{+2} \text{th} s_m^+ \quad (55)$$

wherein $\text{tgh} s_m^-(y/b)$ is defined as in Eq. (34), t , n , x/a , and b being substituted by s , m , y/b , and a . Again, we have the final result of Eqs. (37) and (42), with m , $n \in N_a$, B_{mn} from Eq. (44), and

$$A_{nm} = -(-1)^{[(m-1)m+n+1]/2} \frac{a}{b} \frac{E_{mn}}{N_{am}^b}, \quad n \in N_a \quad (56)$$

For the symmetric-antisymmetric part, in Eqs. (37) and (42) A_{nm} and B_{mn} must be taken from Eqs. (56) and (52), with $m \in N_s$ and $m \in N_a$.

D. Explicit Form of Green's Function

For every class of symmetry, we have developed a set of $2k$ inhomogeneous algebraic equations relating the $2k$ moment coefficients M_n^a and M_m^b . The set of equations can best be handled by matrix techniques. In practical applications, the number k of terms to be considered in Eqs. (23) and (30) does of course depend on the frequency range and on the desired precision. The structure of the coefficient matrix used in the analysis of the forced vibration of the free rectangular plate where $m \in N_a$, $n \in N_s$ is given as follows:

$$\begin{bmatrix} 1 & 0 & 0 & A_{01} & A_{03} & A_{05} \\ 0 & 1 & 0 & A_{21} & A_{23} & A_{25} \\ 0 & 0 & 1 & A_{41} & A_{43} & A_{45} \\ B_{10} & B_{12} & B_{14} & 1 & 0 & 0 \\ B_{30} & B_{32} & B_{34} & 0 & 1 & 0 \\ B_{50} & B_{52} & B_{54} & 0 & 0 & 1 \end{bmatrix} \begin{bmatrix} M_0^a \\ M_2^a \\ M_4^a \\ M_1^b \\ M_3^b \\ M_5^b \end{bmatrix} = \begin{bmatrix} f_0^a \\ f_2^a \\ f_4^a \\ f_1^b \\ f_3^b \\ f_5^b \end{bmatrix}$$

with the matrices

$$\begin{aligned} A &= (A_{nm}), \quad M^a = (M_n^a), \quad f^a = (f_n^a) \\ B &= (B_{mn}), \quad M^b = (M_m^b), \quad f^b = (f_m^b) \end{aligned} \quad (57)$$

Eqs. (31) and (37) lead to

$$M^a + AM^b = f^a, \quad BM^a + M^b = f^b \quad (58)$$

and with the unit matrix I to

$$\begin{aligned} M^a &= (I - AB)^{-1} f^a - A(I - BA)^{-1} f^b \\ M^b &= -B(I - AB)^{-1} f^a + (I - BA)^{-1} f^b \end{aligned} \quad (59)$$

Inserted in Eqs. (24), (31), (48), and (54), we have for the four parts of Green's function of the free rectangular plate

$$\begin{aligned} g_{ij}^f(x, y; \xi, \rho) &= \sum_{m \in N_i} \sum_{n \in N_j} \left[F_{mn} W_m^s(x) W_n^s(\xi) U_n^s(y) U_n^s(\rho) \right. \\ &\quad + W_m^s(x) Y_{jm}(y) \left\langle - (B(I - AB)^{-1})_{mn} U_n^s(\rho) \sum_{p \in N_i} C_{np} W_p^s(\xi) \right. \\ &\quad + \sum_{p \in N_i} ((I - BA)^{-1})_{mp} W_p^s(\xi) D_{pn} U_n^s(\rho) \left. \right\rangle \\ &\quad + X_{in}(x) U_n^s(y) \left\langle \sum_{p \in N_j} ((I - AB)^{-1})_{np} U_p^s(\rho) C_{pm} W_m^s(\xi) \right. \\ &\quad \left. - (A(I - BA)^{-1})_{nm} W_m^s(\xi) \sum_{p \in N_j} D_{mp} U_p^s(\rho) \right. \left. \right] \\ &\quad i, j \in \langle s, a \rangle \end{aligned} \quad (60)$$

E. Receptance Matrices

We consider a free plate excited at four arbitrary points $P_k(x_k, y_k)$ by the forces F_k , $k=1-4$, oscillating harmonically with the frequency ω and the amplitudes f_k (see Fig. 6). Then, the elements of the corresponding receptance matrix are defined as

$$w(x_k, y_k) = H_{kl}^f f_l \quad (61)$$

With Eqs. (11), (12), and (60), from Eq. (61), we have

$$H_{kl}^f = H^f \left(\frac{x_k}{a}, \frac{y_k}{b}, \frac{x_l}{a}, \frac{y_l}{b}, \bar{\eta} \right) = g^f(x_k, y_k, x_l, y_l) \quad (62)$$

The elements H_{kk} define driving-point receptances; deflection and force are measured at the same point. For $x_1=0.7a$ and $y_1=0.8b$, H_{11}^f is given in Fig. 7 as a function of $\bar{\eta}$. The graph is monotonously increasing, which is a general property of the *driving-point* receptances.⁷ The elements H_{kl} , $k \neq l$, can be identified as transfer receptances; deflection and force are measured at different points. For $x_2=-x_1=-0.7a$, $y_2=-y_1=-0.8b$, $H_{12}^f(\eta)$ is given in Fig. 8.

IV. Green's Function for the Free Rectangular Plate Reinforced by a Beam

Using the methods of the substructure technique for continuous systems, we divide the structure into two substructures, following Fig. 1.

First, let us consider the beam loaded by a transverse force per unit length $-p(x)$ and a torque per unit length $m(x)$.

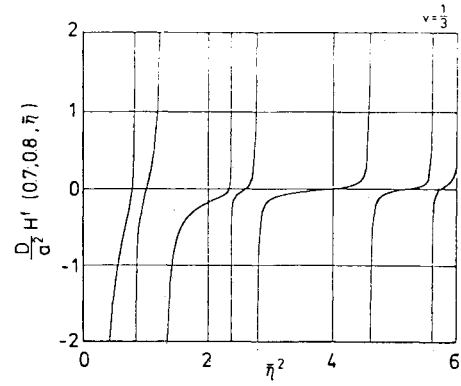


Fig. 7 Driving-point receptance H_{kk}^f over the frequency $\bar{\eta}^2$.

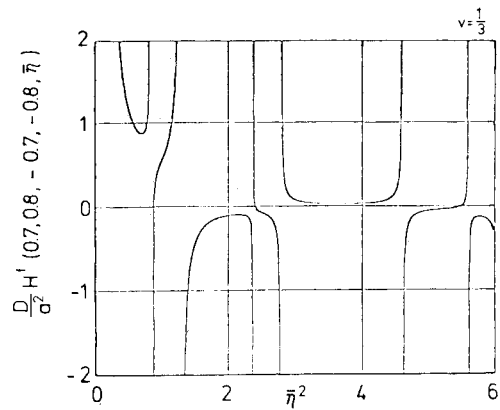


Fig. 8 Transfer receptance H_{kl}^f over the frequency $\bar{\eta}^2$.

For its deflection, with Eq. (8), we get⁸

$$W(x) = - \int_{-a}^a G^f(x, \xi) p(\xi) d\xi \quad (63)$$

and for its torsion,

$$\phi(x) = \int_{-a}^a G_\tau^f(x, \xi) m(\xi) d\xi \quad (64)$$

with Green's function for the free torsion bar

$$\begin{aligned} G_\tau^f(x, \xi) &= \frac{a}{GI_\tau \eta_\tau} \left[\frac{\cos \eta_\tau [1 - (\xi/a)]}{\sin 2\eta_\tau} \cos \eta_\tau \left(1 + \frac{x}{a} \right) \right. \\ &\quad \left. + \sin \eta_\tau \frac{x - \xi}{a} u(x - \xi) \right] \\ \eta_\tau &= a\omega\sqrt{\rho/G} \end{aligned} \quad (65)$$

wherein ρ denotes the density and GI_τ the torsional stiffness.

For the deflection of the second substructure, the rectangular plate loaded by a transverse force per unit area $f(x, y)$, a transverse force per unit length $p(x)$ and a torque $-m(x)$ at the line $y=b$, we have³ with Eqs. (11), (12), and (60),

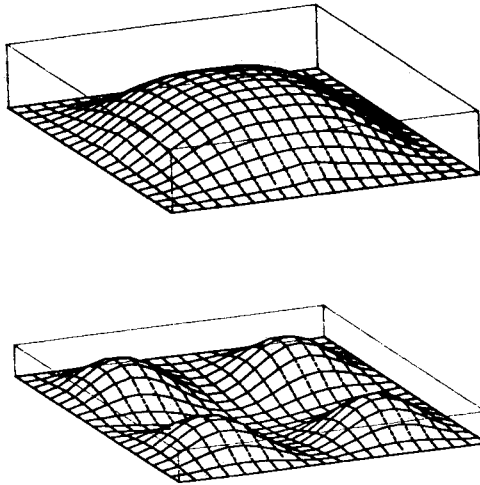


Fig. 9 Symmetric-symmetric modes for the cross-stiffened clamped plate.

$$\begin{aligned}
 w(x, y) &= \int_{-a}^a \int_{-b}^b g^f(x, y, \xi, \rho) [f(\xi, \rho) + p(\xi) \delta(\rho - b) \\
 &\quad + m(\xi) \delta(\rho - b)] d\xi d\rho \\
 &= \int_{-a}^a \left[g^f(x, y, \xi, b) p(\xi) - \frac{\partial}{\partial \rho} g^f(x, y, \xi, b) m(\xi) \right. \\
 &\quad \left. + \int_{-b}^b g^f(x, y, \xi, \rho) f(\xi, \rho) d\rho \right] d\xi \quad (66)
 \end{aligned}$$

and for the geometrical transfer conditions at the coupling line $y = b$,

$$\begin{aligned}
 \underbrace{\begin{bmatrix} W(x) \\ \phi(x) \end{bmatrix}}_{\mathbf{q}(x)} &= - \int_{-a}^a \underbrace{\begin{bmatrix} G^f(x, \xi) & 0 \\ 0 & G_\tau^f(x, \xi) \end{bmatrix}}_{\mathbf{H}_B^f(x, \xi)} \underbrace{\begin{bmatrix} p(\xi) \\ -m(\xi) \end{bmatrix}}_{\mathbf{Q}(\xi)} d\xi \\
 &= \begin{bmatrix} w(x, b) \\ \frac{\partial}{\partial y} w(x, b) \end{bmatrix} \\
 &= \int_{-a}^a \left\langle \int_{-b}^b \underbrace{\begin{bmatrix} g^f(x, b, \xi, \rho) \\ \frac{\partial}{\partial y} g^f(x, b, \xi, \rho) \end{bmatrix}}_{\mathbf{g}^f(x, \xi, \rho)} f(\xi, \rho) d\rho \right. \\
 &\quad \left. + \underbrace{\begin{bmatrix} g^f(x, b, \xi, b) & \frac{\partial}{\partial \rho} g^f(x, b, \xi, b) \\ \frac{\partial}{\partial y} g^f(x, b, \xi, b) & \frac{\partial^2}{\partial y \partial \rho} g^f(x, b, \xi, b) \end{bmatrix}}_{\mathbf{H}_p^f(x, \xi)} \times \begin{bmatrix} p(\xi) \\ -m(\xi) \end{bmatrix} \right\rangle d\xi \quad (67)
 \end{aligned}$$

From Eq. (67), we get an implicit equation for \mathbf{Q} :

$$\begin{aligned}
 \int_{-a}^a [\mathbf{H}_p^f(x, \xi) + \mathbf{H}_B^f(x, \xi)] \mathbf{Q}(\xi) d\xi \\
 = - \int_{-a}^a \int_{-b}^b \mathbf{g}^f(x, \xi, \rho) f(\xi, \rho) d\xi d\rho \quad (68)
 \end{aligned}$$

Now, we develop $\mathbf{Q}(\xi)$ in Fourier series [compare Eq. (23)] as

$$\mathbf{Q}(\xi) = \sum_{m=0}^{k-1} \mathbf{Q}_m W_m^s(\xi) \quad (69)$$

and integrate Eq. (68) multiplied by $W_q^s(x)$, $q = 0, 1, \dots, k-1$, over x as

$$\begin{aligned}
 \sum_{m=0}^{k-1} \left\{ \int_{-a}^a \int_{-a}^a [\mathbf{H}_p^f(x, \xi) + \mathbf{H}_B^f(x, \xi)] W_q^s(x) W_m^s(\xi) dx d\xi \right\} \mathbf{Q}_m \\
 = - \int_{-a}^a \int_{-b}^b \underbrace{\left[\int_{-a}^a \mathbf{g}^f(x, \xi, \rho) W_q^s(x) dx \right]}_{\mathbf{g}_q^f(\xi, \rho)} f(\xi, \rho) d\xi d\rho \quad (70)
 \end{aligned}$$

$q = 0, 1, 2, \dots, k-1$

With

$$\mathbf{g}^f = (\mathbf{g}_q^f), \quad \mathbf{H}_{PB}^f = (\mathbf{H}_{PB, qm}^f), \quad \mathbf{Q} = (\mathbf{Q}_m) \quad (71)$$

we have

$$\mathbf{Q} = - \int_{-a}^a \int_{-b}^b (\mathbf{H}_{PB}^f)^{-1} \mathbf{g}^f(\xi, \rho) f(\xi, \rho) d\xi d\rho \quad (72)$$

and with

$$\begin{aligned}
 \int_{-a}^a \underbrace{\begin{bmatrix} g^f(x, y, \xi, b) \\ \frac{\partial}{\partial y} g^f(x, y, \xi, b) \end{bmatrix}}_{\mathbf{g}^f(x, y, \xi)}^T \begin{bmatrix} p(\xi) \\ -m(\xi) \end{bmatrix} d\xi \\
 = \sum_{m=0}^{k-1} \left[\int_{-a}^a \underbrace{\mathbf{g}^f(x, y, \xi)}_{\mathbf{g}_m^f(x, y)} W_m^s(\xi) d\xi \right]^T \mathbf{Q}_m \quad (73)
 \end{aligned}$$




finally, from Eq. (66)

$$w(x, y) = \int_{-a}^a \int_{-b}^b g(x, y, \xi, \rho) f(\xi, \rho) d\xi d\rho \quad (74)$$

with Green's function for the structure (plate reinforced by beam),

$$g(x, y, \xi, \rho) = \mathbf{g}^f(x, y, \xi, \rho) - \mathbf{g}^{fT}(x, y) (\mathbf{H}_{PB}^f)^{-1} \mathbf{g}^f(\xi, \rho) \quad (75)$$

Table 1 Dimensionless natural circular frequencies λ^2 for a stiffened square plate

Stiffener arrangement	Simply supported		Clamped	
	Present study	Ref. 10	Present study	Ref. 10
	19.76		35.98	
	41.12	41.41	56.82	82.39
	53.63	54.10	67.06	117.13

V. Numerical Results and Comparisons with Other Methods

A comparison of the exact displacement method, the finite-element method, and the lumped mass method concerning the free vibrations of space frames is given by Henshell and Warburton.⁹ They found by numerical experiment that the appropriate choice of method depends upon the number of independent displacements of the structure and the capacity of the computer employed. For a truss structure Poelaert⁵ shows that the finite-element approach results in a relative error of 4% on the frequency and up to 100% on the participation vector compared with the exact method for the same number of independent displacements. The latter error is summed in a repetitive structure.

In contrast to the beam, a closed form cannot be formulated for Green's function of the rectangular plate. For practical purposes, the infinite series in Eq. (60) must be truncated, i.e., the accuracy of the method depends on the number of terms used in the expansion. To compare with available results of the finite-element and finite-difference methods, the case of the simply supported plate is considered for numerical application. Therefore, we have [compare Eqs. (18) and (19)]

$$g^h(x, \xi, y, \rho) = \sum_{m=1}^{\infty} \sum_{n=1}^{\infty} 4F_{mn} W_m^h(x) W_n^h(\xi) U_n^h(y) U_n^h(\rho)$$

$$W_m^h(x) = \sqrt{2} \cos \frac{m}{2} \pi \frac{x}{a}, \quad m \in N_a$$

$$= \sqrt{2} \sin \frac{m}{2} \pi \frac{x}{a}, \quad m \in N_s \setminus \{0\} \quad (76)$$

For $EI/2aD = 10$, $\mu/2a\bar{\mu} = 0.1$, $GI_T/2aD = 0$, and $a = b$, the frequency parameter

$$\lambda_{ss1}^2 = (2a)^2 \Omega_{ss1}^2 \sqrt{\bar{\mu}/D} \quad (77)$$

for the first symmetric-symmetric mode (Ω_{ss1} denotes the corresponding natural circular frequency) for both simply supported and clamped plates stiffened with various numbers of beams is given in Table 1. The clamped plate was modeled by the simply supported plate with four stiffeners resistant to torsion along the edges. Ten terms were taken into consideration in Eq. (76). The comparison with the results of Shastry and Rao,¹⁰ who used 18 high precision plate bending elements for the quarter-plate, shows good agreement for simple support but considerable differences for the clamped plate.

For $EI/2aD = 6$, $\mu/2a\bar{\mu} = 0.05$, $GI_T/2aD = 0.3$, and $a = b$, the frequency parameters λ_{ss1}^2 , λ_{sa1}^2 , λ_{aa1}^2 , and λ_{ss2}^2 for the cross-stiffened plate are given in Table 2. Comparison with the results of Aksu,¹¹ who used the finite-difference technique, shows good agreement except the first symmetric-symmetric mode for the clamped plate. The values of Aksu are lower; but his results assume that a smaller step width would lift the values. In addition the values for the non-stiffened plate are given (see also Gorman¹²). The cor-

Table 2 Dimensionless natural circular frequencies λ^2 for cross-stiffened square plates

Stiffener arrangement		Cross stiffened	
		Present study	Ref. 11
Simply supported	λ_{ss1}^2	19.76	46.72
	λ_{sa1}^2	49.39	90.64
	λ_{aa1}^2	79.02	87.38
Clamped	λ_{ss1}^2	35.98	62.74
	λ_{sa1}^2	73.40	120.30
	λ_{aa1}^2	108.20	118.20
	λ_{ss2}^2	131.92	164.20

responding first two symmetric-symmetric modes for the cross-stiffened clamped plate are shown in Fig. 9.

VI. Concluding Remarks

It has been shown how to handle one- and two-dimensional continuous systems for elements of a dynamical structure. The starting point for substructure technique is Green's function of the continuous system with free edges, which for the beam is given in closed form, for the circular plate as a single,⁶ and for the rectangular plate as a triple Fourier series.

In addition to the coupling of a plate and a beam handled here, the coupling of two or more plates forming for example, a transmission housing, would be of great interest.

References

- ¹Bishop, R. E. D. and Johnson, D. C., *The Mechanics of Vibration*, Cambridge University Press, Cambridge, 1960.
- ²Kouloušek, V., *Dynamics in Engineering Structures*, Butterworths, London, 1973.
- ³Wittrick, W. H. and Williams, F. W., "A General Algorithm for Computing Natural Frequencies of Elastic Structures," *The Quarterly Journal of Mechanics and Applied Mathematics*, Vol. 24, 1971, pp. 263-284.
- ⁴Åkesson, B. A., "PFVIBAT—A Computer Program for Plane Frame Vibration Analysis by an Exact Method," *International Journal for Numerical Methods in Engineering*, Vol. 10, 1976, pp. 1221-1231.
- ⁵Poelaert, D., "DISTEL—A Distributed Element Program for Dynamic Modeling," Proceeding of the 4th VPI&SU/AIAA Symposium on Dynamics and Control of Large Structures, Blacksburg, VA, June 1983, pp. 319-338.
- ⁶Hagedorn, P., Kelkel, K., and Wallaschek, J., *Vibrations and Impedances of Rectangular Plates with Free Boundaries, Lecture Notes in Engineering*, Vol. 23, Springer, Berlin, 1986.
- ⁷Hagedorn, P. and Taliaferro, S., "Some Remarks on Dynamic Receptance, Stiffness and Impedance of Mechanical Systems," *Journal of Applied Mathematics and Physics (ZAMP)*, Vol. 37, Jan. 1986, pp. 134-149.
- ⁸Kelkel, K., "GREENsche Funktion und Impedanz bei Schwingungsproblemen," *Proceedings of the Workshop on the Road-Vehicle-System and Related Mathematics*, edited by H. Neunzert, Teubner, Stuttgart, Federal Republic of Germany, 1985, pp. 79-91.
- ⁹Henshell, R. D. and Warburton, G. B., "Transmission of Vibration in Beam Systems," *International Journal of Numerical Methods in Engineering*, Vol. 1, 1969, pp. 47-66.
- ¹⁰Shastry, B. P. and Rao, G. V., "Vibrations of Thin Rectangular Plates with Arbitrarily Oriented Stiffeners," *Computers and Structures*, Vol. 7, 1977, pp. 47-66.
- ¹¹Aksu, G., "Free Vibration Analysis of Cross Stiffened Rectangular Plates," *Middle East Technical University Journal of Pure and Applied Sciences*, Vol. 9, 1976, pp. 209-226.
- ¹²Gorman, D. J., *Free Vibration Analysis of Rectangular Plates*, Elsevier, New York, 1982.